

conclusions directly applicable to phenomena in three-dimensional crystals<sup>7</sup> cannot be drawn at this time. It does not seem possible to extend these calculations to two or three dimensions by the use of the present, or similarly simple, methods: we have been unable to generalize the simple representation (4) of the lattice sum (3) to higher dimensions. Representations, obtained by the use of theta functions, do exist<sup>9</sup> and pro-

<sup>9</sup> M. Born and M. Bradburn, Proc. Cambridge Phil. Soc. **39**, 104 (1942).

vide a good starting point for numerical work; but they do not provide one with a comparably simple expansion of the dispersion relation about the critical points which are required for an investigation of the resulting singularities. Although one may conclude from these representations that the behavior of the dispersion relation will differ from the usual quadratic one, we have been unable to determine the precise effect on the frequency distribution from them. A detailed investigation of these "unusual" singularities in three dimensions would be of considerable significance.

## Thermoelectric Power of Dilute Indium-Lead and Indium-Thallium Alloys\*†

W. J. TOMASCH AND J. R. REITZ  
Case Institute of Technology, Cleveland, Ohio  
(Received March 24, 1958)

An earlier investigation of the thermoelectric power of dilute ( $\alpha$ -phase) indium-lead alloys, measured relative to pure indium, indicated that there is detailed structure superimposed on the smooth trend of the data. This investigation is now extended to include some twenty-two indium-lead alloys as well as thirteen indium-thallium alloys. For the indium-lead alloys, the existence of structure at both 273°K and 77°K is reaffirmed. On the other hand, the thermoelectric power of the indium-thallium system is found to be an extremely smooth function of the composition in the same range of solute concentration. As a consequence, it is concluded that the observed structure in indium-lead is due exclusively to changes in electronic concentration brought about by alloying.

An estimate of the pure electronic concentration contribution to the thermoelectric power is obtained by subtracting the indium-thallium data from the corresponding indium-lead data. The results of this procedure are demonstrated to be in qualitative agreement with the predictions of a band-model theory which is developed for this comparison. It is therefore suggested that the observed structure can be attributed to the extinction of bands of electron holes and the initiation of bands of overlap electrons. Furthermore, as the result of comparing the thermoelectric data with lattice spacing information, definite suggestions are made concerning the band configuration of pure indium and the evolution of said configuration with alloying. Finally, a very qualitative explanation is offered for the novel face-centered tetragonal ( $c/a > 1$ ) to face-centered tetragonal ( $c/a < 1$ ) phase transformation which occurs at the  $\alpha$ -phase solubility limit.

### I. INTRODUCTION

**I**n general, the addition of a solute impurity differing in valence from the solvent metal produces three important changes relative to conditions existing in the pure solvent: the concentration of nonlocalized electrons changes, thereby changing the Fermi-level; the coupling of such electrons to the lattice changes because of increased impurity scattering, thereby changing the electronic relaxation times; and the strains introduced by the addition of foreign ion-cores cause a relaxation of the Fermi-surface. (This last effect will be assumed quite small by comparison and consequently ignored. In the future, the remaining two effects will be referred

to as the electronic concentration effect and the lattice effect, respectively.)

Recent work on the composition dependence of the thermoelectric power of dilute magnesium alloys, as measured relative to pure magnesium, indicates that the lattice and electronic concentration effects may be separated by considering the two contributions to be algebraically additive.<sup>1</sup> Thus, for example, the electronic concentration contribution for a magnesium-indium alloy of a given atomic percent composition is obtained by subtracting the observed thermoelectric power of a magnesium-cadmium alloy of identical atomic composition from the observed value for the magnesium-indium alloy. According to this scheme, the thermoelectric power of the magnesium-cadmium alloy system represents, to some degree of approximation, the lattice contribution associated with the solutes of the fifth period of the periodic table.

\* This work was supported in part by The National Carbon Company (Division of Union Carbide Corporation), and in part by the Office of Naval Research.

† This paper is part of a thesis submitted by W. J. Tomasch in partial fulfillment of the requirements for the degree of Doctor of Philosophy. A major portion of the measurements were made while he was a Standard Oil Fellow (Standard Oil Company of Ohio).

<sup>1</sup> Salkovitz, Schindler, and Kammer, Phys. Rev. **105**, 887 (1957).

Similar measurements using indium as the solvent metal are reported here by the authors. A scheme analogous to the one just outlined is used in an attempt to isolate the electronic concentration contribution to the thermoelectric power. It is possible to interpret the final results in terms of the band-model approximation.

## II. EXPERIMENTAL SITUATION

Figure 1 indicates the basic thermoelectric circuit used to measure the thermoelectric power of indium alloys relative to pure indium. It consists of a pure indium wire soldered to an indium alloy wire, thereby forming a hot junction, and copper voltage leads soldered to the other ends of these wires, thereby forming two cold junctions. The temperatures of the cold junctions are fixed at a common value ( $T_1$ ) by immersion in a constant-temperature cold bath consisting of either boiling liquid nitrogen or melting ice, while the hot junction can be raised to a higher temperature ( $T_2$ ) by means of an electric heater. Copper-constantan thermocouples are soldered to the hot junction and to one of the cold junctions for the purpose of measuring the temperatures at these points. The copper wires from the cold junctions serve as input leads for a high-impedance ( $13 \times 10^6$  ohms) recording dc amplifier.<sup>2</sup> It is possible therefore to measure the emf developed as a function of the temperature difference, the initial slope of this emf-temperature curve being the thermoelectric power at  $T_1$ . At no time during the course of the measurements did the dc amplifier's input circuit draw more than  $2 \times 10^{-13}$  ampere from the thermocouple.

The cryostat used to produce the proper thermal environment for the indium-alloy thermocouples has two important features: hot and cold junctions are situated in approximately isothermal surroundings, and the thermal gradient achieved over the remaining length of the thermocouple wires is essentially constant.

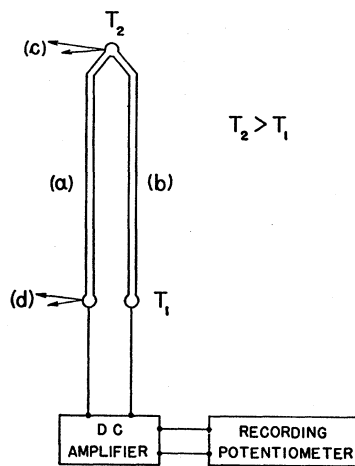


FIG. 1. Schematic diagram of circuit used to measure the thermoelectric power of indium alloys relative to pure indium: (a) alloy wire, (b) pure indium wire, (c) hot junction monitoring thermocouple, and (d) cold junction monitoring thermocouple.

The first of these removes the possibility of influencing the measurements through the presence of soldered connections at the junctions. If local inhomogeneities are present in the wires, e.g., those due to crystalline anisotropy, the second feature assures a uniform averaging process in which no local element of the thermocouple is overemphasized by the thermal gradient. A generous length for the thermocouple wires themselves, about twenty centimeters or roughly one hundred times the length of a single crystallite, allows such an averaging process to be effective. Attention to all these factors is known to be important from experience with other cryostat designs. As a result of explicit tests, as well as long term experience, it is believed that the design utilized for the measurements here reported adequately satisfies the aforesaid conditions, and that the data do not depend significantly on the operating parameters of the cryostat.

## III. ALLOY PREPARATION

All alloys are prepared from pre-outgassed constituents by a vacuum casting technique which is now described. The alloy constituents are placed in a Pyrex tube crucible whose interior has been coated with a vacuum-baked layer of colloidal graphite to prevent the finished ingot from welding itself to the glass walls. A mechanical vacuum pump is connected to the crucible which is then inserted into a tight-fitting electric tube furnace ( $\sim 400^\circ\text{C}$ ) where it remains for about twenty minutes. The crucible is agitated vigorously several times during this period so as to achieve mixing of the constituents, all of which are molten at the indicated temperature. After this period, the crucible is removed from the furnace and quenched in water. When the ingot is removed, it is covered with a smooth layer of carbon which disengages itself in large flakes upon immersion in concentrated nitric acid. After washing, the ingots are ready for extrusion into wire. The outgassed alloy constituents are prepared from spectroscopically pure metals by a process quite similar to that just described. This procedure is observed to remove dissolved gasses and reduce oxidation in the final alloy ingots.

Wires of pure indium (99.999%) and indium alloy forty mils in diameter are manufactured by means of a stationary billet extrusion process. Only one wire is produced from a given die set to eliminate possible contamination problems and as a matter of convenience.

## IV. VALIDITY OF DATA

A number of factors bear heavily on the validity of the thermoelectric power measurements and therefore must be investigated in an explicit fashion. Effects due to the cryostat have been mentioned earlier so that only effects produced by shortcomings of the thermocouple wire themselves need be considered. Several possible defects come to mind immediately: contamina-

<sup>2</sup> Leeds & Northrup No. 9835 synchronous chopper amplifier in series with a type-H recording potentiometer.

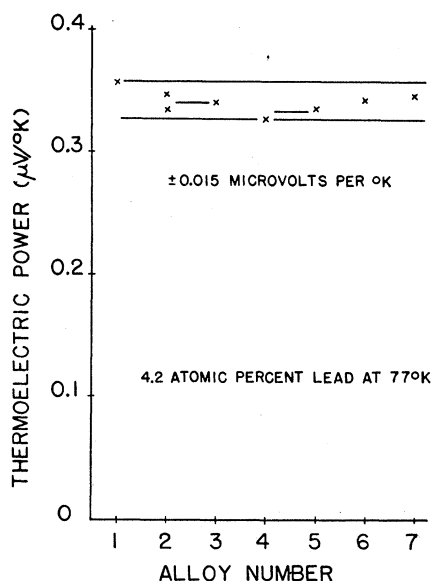


FIG. 2. Reproducibility data obtained from seven indium-lead alloys of the same intended composition (4.2 atomic percent lead). Positive thermoelectric powers correspond to electron flow from the alloy to the pure indium at the hot junction. The two data points for alloy number two are indicative of the scatter encountered when an alloy-indium thermocouple is removed from the cryostat and then reinstalled.

tion due to alloying techniques, solute inhomogeneities, excessive stressing, and deviations from intended composition. With regards to chemical composition, several chemical analyses indicate that deviations are sufficiently small so as to warrant use of the intended compositions. This is in agreement with the conclusions of other workers.<sup>3</sup>

The aforesaid analyses also indicate that the net contamination of a sample lies below about 0.05 mass percent. Other tests also display the absence of appreciable contamination due to metallurgical techniques of alloy manufacture. Combustion analysis of vacuum-outgassed indium discloses the presence of less than 0.05 mass percent carbon. A thermocouple consisting of one wire of spectroscopically pure indium (99.999% pure) just as it is received from the supplier, and the other of vacuum-outgassed indium, displays no thermoelectric power to within the accuracy claimed for such measurements. One further precaution can be taken with respect to contamination; indium from the same vacuum cast ingot can be used to manufacture both the alloy wire and the indium wire of a thermocouple. This tends to cancel effects due to contamination of the pure indium ingot.

Homogeneity can be tested by making two thermocouples, each using a wire made from half a single double-sized alloy ingot, i.e., one from the top half and the other from the bottom. Such experiments yield

<sup>3</sup> Moore, Graham, Williamson, and Raynor, *Acta Met.* 3, 580 (1955).

the same values for the two thermoelectric powers within the experimental error claimed, thus establishing the adequate homogeneity of the samples.

Tests conducted on annealing disclose that the major effects of the extreme cold work produced by extrusion are removed by annealing the samples for about an hour at 130°C. As a practical matter, all alloys used were annealed from twelve to seventeen hours at about 130°C.

Figure 2 presents the results of measurements made at 77°K for seven indium-lead alloys of the same intended solute concentration (4.2 atomic percent). The lower temperature is chosen since the over-all reproducibility is observed to be somewhat poorer at 77°K than at 273°K. Alloys number two and three together with four and five are manufactured from halves of double-sized ingots as mentioned earlier. Only alloys six and seven are prepared by the continuous pumping, carbon crucible process previously discussed. The remainder are prepared by sealing the alloy constituents (not outgassed) in evacuated Pyrex ampules which are then placed in an electric oven (~400°C). Better mixing can be achieved by this method since the molten charge can be agitated violently without danger of loss or freezing. Defects of the method consist of the light scumming at the ingot tops presumably due to small amounts of oxidation, and a tendency for the ingots to weld themselves to the glass walls of the ampule. The maximum spread of the data of Fig. 2 corresponds to an uncertainty of  $\pm 0.015$  microvolt per °K and this degree of accuracy is considered to be adequate. The over-all agreement between these seven values is taken as strong indication that all essential experimental variables are being satisfactorily controlled.

## V. THERMOELECTRIC POWER DATA

Results of measurements made on thirteen indium-thallium alloys and twenty-two indium-lead alloys are presented in Figs. 3 and 4. (Much of the information

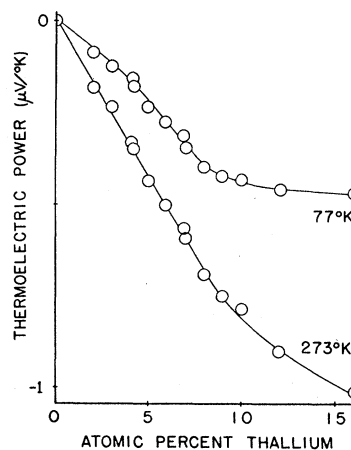


FIG. 3. Thermoelectric power of the indium-thallium system vs pure indium as a function of composition.

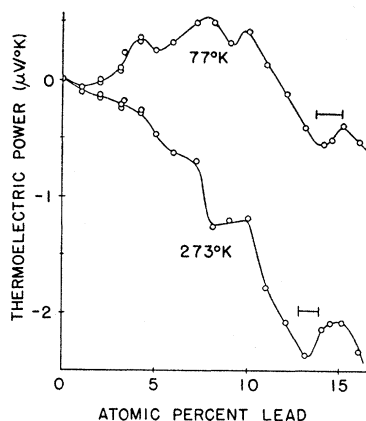


FIG. 4. Thermoelectric power of the indium-lead alloy system vs pure indium as a function of composition. Two-phase transition regions are indicated with bars.

presented in Fig. 4 has been reported earlier.<sup>4</sup>) The detailed structure superimposed on the smooth trend of the indium-lead data is considerably larger than can be accounted for by the experimental uncertainties just discussed. It can also be argued that the comparative smoothness of the indium-thallium data suggests strongly that such an explanation is unlikely. In addition, certain regularities in the aforesaid structure serve to increase confidence in the essential correctness of the measurements. The maxima (77°K and 273°K) occurring beyond thirteen atomic percent lead are associated with the face-centered tetragonal ( $c/a > 1$ ) to face-centered tetragonal ( $c/a < 1$ ) phase transformation which is known to take place in the indicated composition ranges.<sup>5</sup> It is reassuring to note in the manner in which the phase change is traced out by different data points for the two temperatures involved. Before the availability of the complete indium-thallium data, attempts were made to correlate the 77°K and 273°K structural details by interpreting the structure in terms of positive thrusting peaks superimposed on a smooth variation. Such interpretation leads to the conclusion that raising the temperature causes the peaks to move toward lower lead concentrations as well as making them "wash out," the latter effect becoming more pronounced with decreasing lead concentration. In fact, the peak occurring at roughly four atomic percent lead must be assumed totally washed out by 273°K. Subsequent information has led to the reinterpretation of the structure in terms of negative thrusting peaks or dips. (Reasons for preferring such an interpretation will emerge from later discussion.) Hence, for the lower temperature, the structure consists of two dips rather than three peaks. Both dips are also present at 273°K, and no net trends seem to be indicated in the sense of concentration shifts or "washing out." Again it can be pointed out that the dips are traced out by different data points for the two temperatures.

In view of these considerations, it is believed that

<sup>4</sup> W. J. Tomasch, Phys. Rev. **109**, 69 (1958).

<sup>5</sup> See reference 3, p. 586.

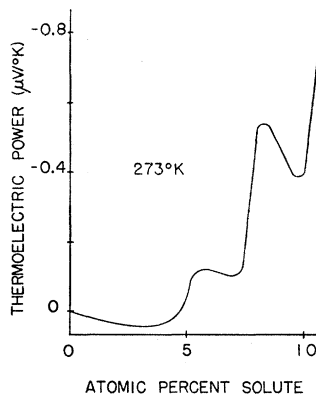


FIG. 5. Thermoelectric power of the indium-lead system minus that of the indium-thallium system as a function of solute concentration.

the existence of the detailed structure has been reasonably well established.

## VI. INTERPRETATION OF STRUCTURE

### A. General

Thallium has the same valence as indium (3), and indium-thallium alloys display no structure in the concentration variation of the thermoelectric power. Lead has a greater valence than indium (4), and indium-lead alloys exhibit structure. An obvious interpretation of these facts is that the structure arises from an increase in electronic concentration. If this is indeed the case, it is to be hoped that the structural details of the thermoelectric power data may shed light on the band structure of these alloys as well as on that of pure indium itself. To this end, it is helpful to follow the suggestion mentioned earlier.<sup>1</sup>

According to this suggestion, the electronic and lattice contributions to the thermoelectric power of the indium-lead alloys may be separated by considering the two effects to be algebraically additive. Since thallium and lead lie adjacent to one another in the same period of the periodic table, it is further suggested that the lattice contribution for thallium and lead may be similar. Hence it is possible to obtain an approximation to the electronic concentration contribution for an indium-lead alloy of a given solute concentration by subtracting the thermoelectric power of an indium-thallium alloy of identical solute concentration from that of the indium-lead alloy. Figure 5 displays the result of subtracting the 273°K indium-thallium data from the corresponding indium-lead data. Due to the increased difficulty in interpreting intermediate temperature thermoelectric data, said difficulty being generally encountered when the temperatures involved are no longer large compared to about one quarter of the Debye temperature, a curve similar to Fig. 5 and corresponding to the 77°K measurements has been omitted. (Changes in the nature of the electron-phonon scattering process are presumed to be basically responsible for this situation. In the intermediate-temperature range, solutions based on a relaxation

time may no longer satisfy the Boltzmann transport equation.) The principal function of the 77°K data has been to confirm the structure observed at 273°K.

There are two main features displayed by the curve of Fig. 5: a rather long interval (0–5 atomic percent) during which the thermoelectric power remains relatively unchanged, followed by three more or less sharp negative thrusting breaks. If Fig. 5 does indeed present the essential nature of the electronic contribution to the thermoelectric power, it may be possible to understand its main features in terms of a simple band model.

### B. Band-Model Approximation

It is known that the relative thermoelectric power ( $\mathcal{E}$ ) associated with two materials can always be expressed as the difference of their absolute thermoelectric powers ( $S$ ).<sup>6</sup> Thus,

$$\mathcal{E}_{AM} = S_A - S_M, \quad (1)$$

where  $A$  and  $M$  refer to alloy and pure solvent metal, respectively. The band-model approximation yields the following equation for the absolute thermoelectric power of a solid<sup>7</sup>:

$$S = -\frac{1}{|e|} \frac{\pi^2}{3} k^2 T \frac{\partial}{\partial \zeta} \left\{ \ln \sum_i \sigma_i(\zeta) \right\} \\ = -\frac{1}{e^2} K(T) \frac{\partial}{\partial \zeta} \left\{ \ln \sum_i \sigma_i(\zeta) \right\}, \quad (2)$$

where the index  $i$  ranges over all carrier bands present in the solid,  $\sum_i \sigma_i = \sigma$  the total electronic conductivity, and  $\zeta$  is the Fermi level of the solid. (Electronic is used in the sense of both overlap electrons and electron holes.) The other symbols of Eq. (2) have their usual meaning.

Nearly free behavior is assumed for the carriers, so that

$$\sigma_i = n_i e^2 \tau_i / m_i^*, \quad (3)$$

where  $m_i^*$  and  $\tau_i$  are the effective band mass and relaxation time, respectively. The relaxation time referred to is derived from the separate relaxation times associated with the various electronic scattering processes. To some extent, the detailed behavior of the absolute thermoelectric power, as given by Eq. (2), is controlled by the energy dependence of these separate relaxation times. It is assumed that impurity (solute) scattering and thermal lattice scattering are primarily responsible for coupling the carriers to the lattice. The following equations display the energy dependence of the relaxation times for these processes.<sup>8</sup> (For thermal scattering, the energy dependence of the relaxa-

tion time is usually purported to be  $\tau_T \propto \zeta^{\frac{1}{2}}$ , but if the band occupation is less than one-quarter carrier per atom, then  $\tau_T \propto \zeta^{-\frac{1}{2}}$ . The latter stipulation applies to the case at hand.)

$$\tau_I = t_I (\zeta_i / \zeta_{i0})^{-\frac{1}{2}}, \quad (\text{impurity}) \quad (4)$$

$$\tau_T = t_T (\zeta_i / \zeta_{i0})^{-\frac{1}{2}}, \quad (\text{thermal}) \quad (5)$$

where  $\zeta_{i0}$  is the band Fermi energy when the band is in some standard state of occupation. In these equations,  $t_I$  is assumed to be a function of solute concentration only, and  $t_T$  a function of temperature only. It is convenient to write Eq. (2) as the unfactored sum

$$S = \sum_i S_i = -\frac{1}{e^2} K(T) \sigma^{-1} \sum_i \frac{\partial \sigma_i}{\partial \zeta}. \quad (6)$$

The  $S_i$  can be called "partial" absolute thermoelectric powers. These are not quite "band" thermoelectric powers since the influence of other bands is contained in the common factor  $\sigma^{-1}$ .

Equation (1) may be rewritten as

$$\mathcal{E}_{AM} = \sum_i S_{iA} - \sum_i S_{iM} = \sum_i \delta_i S_i. \quad (7)$$

The band approximation solution consistent with the assumptions previously mentioned can be stated in terms of the  $\delta_i S_i$ :

$$\delta_i S_i = -K(T) \{ (\delta_{iA} \beta_{iA} / \sigma_A) - (\delta_{iM} \beta_{iM} / \sigma_M) \}, \quad (8)$$

$$\beta_i = (n_{i0} / m_i^* \zeta_{i0}) (t_I^{-1} + t_T^{-1})^{-1}, \quad (9)$$

where  $n_{i0}$  is the occupation of the band corresponding to  $\zeta_{i0}$ . Since a given species of carrier ( $i$ ) may not be present in both the alloy ( $A$ ) and the pure solvent metal ( $M$ ), it has been necessary to introduce the function  $\delta_i$  into Eq. (8). For overlap electrons:

$$\delta_i = 1 \quad (\text{if species } i \text{ is present}), \\ = 0 \quad (\text{if not}). \quad (10)$$

For electron holes:

$$\delta_i = -1 \quad (\text{if species } i \text{ is present}), \\ = 0 \quad (\text{if not}). \quad (11)$$

As a further consequence of the model, the conductivity of the alloy ( $\sigma_A$ ) may be written as

$$\sigma_A = \sigma_M + \Delta_e \sigma + \Delta_c \sigma + \text{terms of higher order}. \quad (12)$$

The second term of Eq. (12) is due only to changes in electronic concentration caused by alloying, while the third is due only to changes in relaxation time. Also, there is a term (the higher order term) which couples these two effects, but it varies as their product and will be assumed negligible for the composition range studied. At this point, it is convenient to investigate the results of employing the earlier suggestion that subtracting the relative thermoelectric powers of the two alloy systems (each *versus* pure indium) somehow removes the major effects of impurity scattering and

<sup>6</sup> N. F. Mott and H. Jones, *Properties of Metals and Alloys* (Oxford University Press, New York, 1936), p. 309.

<sup>7</sup> See reference 6, p. 310.

<sup>8</sup> A. H. Wilson, *Theory of Metals* (Cambridge University Press, New York, 1954), pp. 269, 264.

leaves only the pure electronic concentration effect. Thus, in comparing the theory with Fig. 5, it will be necessary to delete all  $\Delta_c$ -type terms wherever they occur. Consequently, Eq. (8) may be written as

$$\delta S_i = -K(T)\beta_{iM}\{(\delta_{iA}/\sigma_A') - (\delta_{iM}/\sigma_M)\}, \quad (13)$$

where

$$\sigma_A' = \sigma_M + \Delta_c \sigma.$$

To some extent, since  $\delta S = \sum_i \delta S_i$ , it is possible to look at the behavior of individual bands and then sum the results although in principle this is complicated by the interdependence of the  $\delta S_i$  via  $\sigma$ . There are two most interesting cases to which Eq. (13) may be applied: the extinction of a band of holes, and the initiation of a band of overlaps. For holes:

$$\begin{aligned} \delta S_h &= +K\beta_{hM} \left\{ \frac{1}{\sigma_A'} - \frac{1}{\sigma_M} \right\} \quad (\text{before extinction}), \\ &= +K\beta_{hM} \left\{ 0 - \frac{1}{\sigma_M} \right\} \quad (\text{after}). \end{aligned} \quad (14)$$

For overlaps:

$$\begin{aligned} \delta S_e &= 0 \quad (\text{before initiation}), \\ &= -K\beta_{e0}/\sigma_A' \quad (\text{after}). \end{aligned} \quad (15)$$

The value of  $\beta$  corresponding to the alloy composition at which overlap first occurs is designated  $\beta_{A0}$ .

There is obviously a rather strong similarity between these two cases inasmuch as  $\delta S$  undergoes a step discontinuity of the form  $-K\beta/\sigma$  for each. It is to be hoped that this sort of behavior can be invoked to explain the sharp breaks of Fig. 5. In order to comment on the behavior of  $\delta S_h$  before extinction or on  $\delta S_e$  after initiation, it is necessary to make some rather special further assumptions. Assuming that  $\sigma_A'$  increases with electron concentration, which is certainly expected for indium alloys, the relative thermoelectric power will tend to vary as indicated in Fig. 6(a) during the

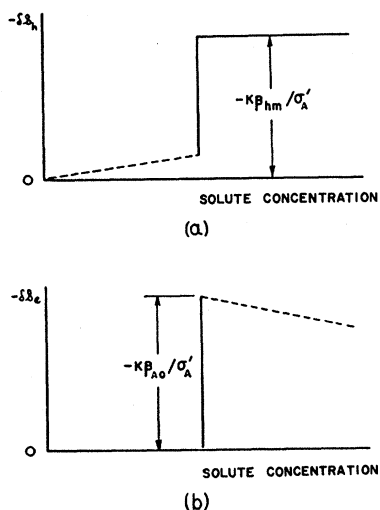


FIG. 6. Predicted behavior of band contributions to the relative thermoelectric power (electronic concentration effect): (a) extinction of a band of holes, (b) initiation of a band of overlap electrons. The broken line portions of these curves indicate regions in which the thermoelectric power varies smoothly with composition, but requires further simplifying assumptions to determine the form of the variation.

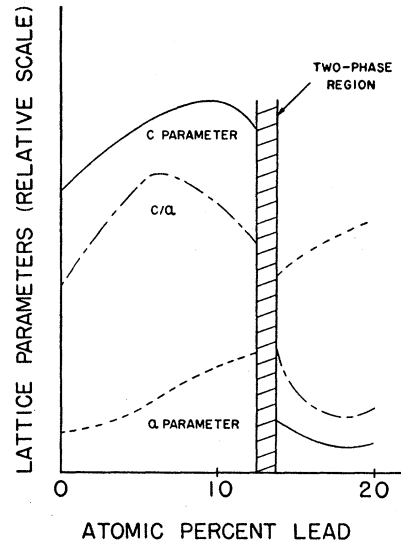


FIG. 7. Schematic parameter-composition curves for the indium-lead alloy system (see reference 3).

extinction of a single band of holes. For overlaps, the new band contribution to the relative thermoelectric power will tend to vary as indicated in Fig. 6(b). A superposition of curves of the general nature displayed in Fig. 6 would indeed appear capable of synthesizing a function with the qualitative features of Fig. 5. It should be remembered that only the *details of behavior* before the extinction of holes or after the initiation of overlaps depend on further simplifying assumptions.

The empirical approximation which allows Eq. (8) to be rewritten as Eq. (13) needs not be adopted as an essential feature of the model. It is possible to apply Eq. (8) and Eq. (12) to the case of the indium-thallium alloy system and then actually form the differences of interest. The net outcome of such an approach is to introduce a multiplicative modulating factor into expressions (14) and (15), said factor being equal to unity for zero solute concentration.<sup>9</sup> It is difficult to discuss the modulation in detail since its particulars depend on a knowledge of many individual band parameters which are not known. It is believed, however, that the modulation is a monotonic function of the concentration, and probably a fairly slowly varying function as well. The monotonic behavior essentially reflects the fact that the indium-thallium data are a monotonic function of solute concentration. All this seems to imply that the curves of Fig. 6 are not to be altered in any profound fashion by discarding the aforementioned approximation.

### C. Specific Interpretations

Although it appears that the main features of Fig. 5 can indeed be interpreted in terms of band extinctions

<sup>9</sup> W. J. Tomasch, thesis, Case Institute of Technology, 1958 (unpublished).

and initiations, there is obviously a practical difficulty in distinguishing between the two processes. In fact, this difficulty cannot be overcome without recourse to extra information concerning other physical properties of indium-lead alloys, and even then the results must be considered to be of a rather speculative nature.

The variation of lattice spacing parameters as function of lead concentration has been carefully studied for indium-lead alloys to slightly beyond the  $\alpha$ -phase solubility limit (see Fig. 7).<sup>10</sup> It could be hoped that a simultaneous band-model explanation of the thermoelectric and the lattice spacing data would uniquely settle the difficulty in question. Unfortunately, however, the latter explanation is by no means a simple matter. A development due to Jones<sup>11</sup> can be used to correlate the lattice spacing information with band effects but this treatment has met with certain objections.<sup>12</sup> Nevertheless, it will be used in an attempt to rationalize the thermoelectric and lattice spacing data. Simply said, it has been suggested that the initiation of an overlap band causes the Brillouin zone to deform as if compressive stresses had been applied across the overlapped zone faces. This results in a contraction along the overlap axis in reciprocal space and a corresponding expansion of the crystal structure in the same direction. Figure 8 schematically depicts the Brillouin zone for a face-centered tetragonal structure. The letters *A*, *C*, and *D* label the three kinds of zone faces; there are four *A*-type faces, two *C*-type faces and eight *D*-type faces. Various band species are also indicated and will be subsequently referred to by the designations listed in the caption.

Figure 9 presents an interpretation of the electronic concentration contribution to the thermoelectric power which is thought to be consistent with lattice spacing

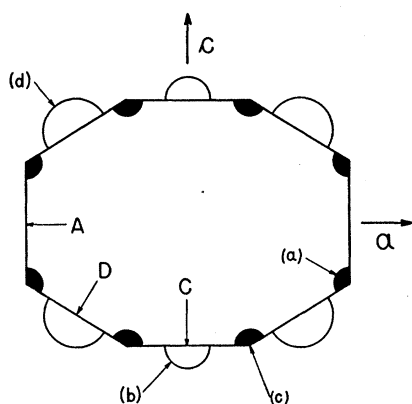


FIG. 8. Schematic representation of the Brillouin zone and suggested band structure for indium: (a) *A*-type holes, (b) *C*-type overlaps, (c) *C*-type holes, and (d) *D*-type overlaps. The letters *A*, *B*, and *C* label the three different kinds of zone faces.

<sup>10</sup> See reference 3, p. 587.

<sup>11</sup> H. Jones, Proc. Roy. Soc. (London) **A147**, 400 (1934); *Physica* **15**, 13 (1949); *Phil. Mag.* **41**, 663 (1950).

<sup>12</sup> J. B. Goodenough, *Phys. Rev.* **89**, 282 (1953); J. W. McClure, *Phys. Rev.* **98**, 449 (1955).

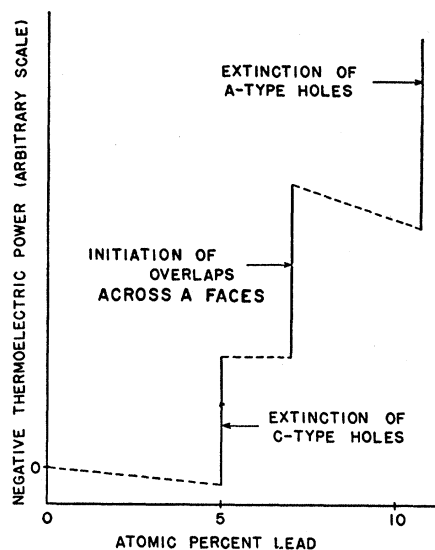


FIG. 9. Proposed band-model explanation for the electronic concentration contribution to the thermoelectric power of indium-lead alloys. (See Fig. 6.)

considerations. As a result of this interpretation, it is proposed that the band structure indicated in Fig. 8 does in fact correspond to the case of pure indium. The suggested interpretation proceeds along lines which are now outlined. From zero to five atomic percent, the main effect of alloying is to fill *C*-type holes. At roughly five atomic percent, the *C*-type holes are completely extinguished and the first negative step discontinuity occurs in  $\delta S_e$  (Fig. 5). Minor changes in the concentration of *A*-type holes and *C*-type overlaps are also assumed to occur in this composition interval as well as in the interval five to seven atomic percent solute. At roughly seven atomic percent, overlaps across the *A* faces are initiated, thereby generating the second step discontinuity. From seven to ten atomic percent, *A*-type holes are rapidly filled until they are completely extinguished at a little beyond ten atomic percent, giving rise to the third and last step discontinuity before reaching the solubility limit. Nothing as yet has been said about the presence of *D*-type overlaps, but their number must certainly increase somewhat with alloying. Translation vectors of the reciprocal lattice can be used to map their eight hemispheres into four complete and similar spheres (bands). In this sense they form four degenerate bands. The effect of changing the occupation of these bands is believed to be rather small because they can never give rise to the relatively large step-discontinuity associated with band initiations or extinctions. Their principal effect probably consists of adding a small net trend to the curve of Fig. 9. Similar comments apply to the influence of *C*-type overlaps.

It is interesting to note in passing that the proposed band pictures can account for indium's tetragonality as well as for the face-centered tetragonal ( $c/a > 1$ ) to

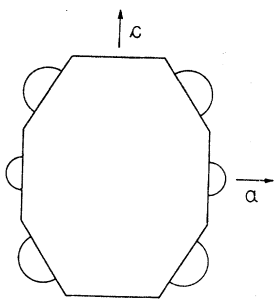


FIG. 10. Suggested band structure for overlap electrons in indium-lead alloys lying just beyond the  $\alpha$ -phase solubility limit.

face-centered tetragonal ( $c/a < 1$ ) phase transformation which occurs at the lead solubility limit ( $\alpha$  phase). The first half of this statement is obviously made in reverse fashion since the tetragonality of indium originally suggested the incorporation of overlaps across  $C$ -type zone faces and not  $A$ -type. As for the rest, it is consistent to suppose that after the phase transformation, overlap occurs across the  $A$ -type faces and not the  $C$ -type, as indicated in Fig. 10. Roughly

speaking, it is suggested that alloying tends to favor those effects which change the direction of easy overlap from the  $c$ -axis to any direction contained by the plane of the  $a$ -axes, so that the *increased* multiplicity of  $A$ -type overlaps can be utilized to reduce the rate at which the Fermi energy increases with alloying. Obviously this is not an "explanation" in any basic sense, but it does supply an intuitive feeling for the way in which the Fermi surface tends to develop with alloying in this alloy system.

#### ACKNOWLEDGMENTS

The authors wish to express their gratitude to Professor Charles S. Smith for numerous discussions which materially aided in surmounting certain experimental difficulties. They would also like to thank Mr. A. Hruschka and the other members of the Physics Department machine shop for their services in manufacturing the cryostat and extrusion dies used in these measurements.

## Cathodoluminescence of Strontium Oxide, Barium-Strontium Oxide, and Magnesium Oxide\*

H. W. GANDY†

*Department of Physics, University of Missouri, Columbia, Missouri*

(Received May 24, 1957; revised manuscript received April 16, 1958)

A survey of some spectral and time decay properties of the cathodoluminescence of SrO, (BaSr)O, and MgO samples has been made in sealed-off high-vacuum tubes in the spectral range from 220  $m\mu$  to 600  $m\mu$ . Observations were made for sample temperatures varying from 90°K to room temperature and above with the samples in different states of thermionic activity.

In SrO samples, luminescence maxima were observed at photon energies of 4.9 ev, 3.7 ev, 3.2 ev, and 2.4 ev. The 4.9-ev band intensity increases with the thermionic activity of the sample whereas that of the 3.2-ev band decreases.

Emission band maxima were found in (BaSr)O at energies of 4.0 ev, 3.1 ev, 2.6 ev, and 2.1 ev. A comparison of the (BaSr)O luminescence is made with that from SrO and BaO.

MgO samples were studied in both polycrystalline and single crystal forms. Luminescence band maxima were observed at energies of 5.2 ev, 3.6 ev, 2.7 ev, 2.3 ev, and 2.1 ev. The 2.3-ev band may be enhanced by heating the sample in magnesium vapor or diminished by heating it in oxygen.

Suggestions are made concerning possible electronic mechanisms giving rise to some of the above bands on the basis of the temperature dependence of their intensities and their types of afterglow.

#### INTRODUCTION

SOME of the alkaline earth oxides are important as thermionic and secondary emitters of electrons when they have been suitably prepared. Since many of the interesting electrical properties of these oxides depend in part upon the presence of crystalline defects and small departures from stoichiometry in these materials, the determination of their extrinsic electronic energy structures associated with these conditions is

desirable. To this end, this investigation is concerned with spectral and time-decay studies of the cathodoluminescence of SrO, (BaSr)O, and MgO samples which were as free from foreign impurities as could be conveniently obtained.

#### Barium-Strontium Oxide and Strontium Oxide

The mixed crystalline material (BaSr)O is a very efficient thermionic emitter and is widely used as a commercial cathode material in electron tubes. It is known that the thermionic activity of this substance

\* Supported by the Office of Naval Research and by a grant from the R.C.A. Laboratories Division, Princeton, New Jersey.

† Now at the General Electric Company, Syracuse, New York.